17th World Conference on Earthquake Engineering, 17WCEE
Sendai, Japan - September 13th to 18th 2020

A CALIBRATED SIMPLIFIED MODEL FOR PLANE AND REGULAR R/C MOMENT RESISTING FRAMES

J. Muñoz[1], J. de la Llera[2], A. Poulos[3], J. Vásquez[4], T. Rossetto[5]

[1] *Researcher, Research Center for Integrated Disaster Risk Management (CIGIDEN), CONICYT/FONDAP/15110017, Santiago, Chile, jp.munoz@cigiden.cl*
[2] *Lead Researcher, Research Center for Integrated Disaster Risk Management (CIGIDEN), CONICYT/FONDAP/15110017, Santiago, Chile, jcllera@ing.puc.cl*
[3] *PhD Candidate, University of Stanford, apoulos@uc.cl*
[4] *Researcher, Research Center for Integrated Disaster Risk Management (CIGIDEN), CONICYT/FONDAP/15110017, Santiago, Chile, jorge.vasquez@cigiden.cl*
[5] *Lead Researcher, EPICentre, t.rossetto@ucl.ac.uk*

Abstract

Because computational time is still a limitation for building inelastic dynamic analysis, an enhanced version of a simplified model for efficient analysis and design of 2D regular moment resistant reinforced concrete frames is proposed herein. The model is an adaptation of the Modified Fishbone Model (MFB) originally developed for steel Moment Resisting Frames. The MFB replaces all elements of a story with a macro-column, a pair of macro-beams, and a pair of vertical truss elements. Both macro-elements consist of elastic members with inelastic end hinges. A new smooth hysteretic model for the rotational springs of the MFB is proposed herein, considering ductility-based stiffness degradation, ductility- and energy-based strength degradation, and pinching. The responses of the MFB are compared against a force-based fiber model, which considers modified Kent-Park and Menegotto-Pinto models for concrete and steel fibers, respectively. The calibration of the MFB considers a set of pushover analyses and the use of the Particle Swarm Optimization/Nelder-Mead algorithm for the parameter identification phase. A set of plane frames of 1, 5, 10, 15 and 20 stories, with 3, 6 and 9 regular bays is studied with consistent seismic records selected by a Conditional Spectrum from the SIBER-RISK ground motion database. The proposed numerical model presents errors that usually are less than 20% and 40% for the mean and standard deviation, respectively, of the peak responses of story displacement and base shear, and requires between 5 to 30 times less computational time than the counterpart fiber model. The results are acceptable for all tested buildings and the precision is better for larger inelastic behavior.

Keywords: simplified model, modified fishbone model, OpenSees, reinforced concrete, optimization

1. Introduction

1.1 Statement of the problem

It is well-known that some countries are prone to large and potentially destructive earthquakes —e.g., Chile, western US, Japan, or Italy. Hence, two very important goals of structural engineers are: (1) to build safe structures; and (2) to evaluate the safety of existing buildings whenever the design code is updated. It is crucial to know whether buildings are safe or not, because when subject to an earthquake there are many potential losses, such as economical ones due to damage of the structure itself or non-structural elements, or due to loss of functionality in critical lifelines such as the transport, electrical, water or health networks [1, 2] where the building is located; and more importantly, due to human casualties. Therefore, given the many assets at stake, it is important that a designer can guarantee that a new building is safe; however, how can an engineer measure the safety of an existing building?

For the case of reinforced concrete buildings, code requirements for steel reinforcement detailing provide conditions for the safety of structural components; however, since the design is obtained with a design spectrum and the actual demand is unknown, it is quite uncertain how "big" the safety margin is. To improve and quantify the safety margin of a building, the engineer typically designs seismic protection systems; or carries out a risk analysis to evaluate new and existing buildings. For the former, one of such methods was recently published [3], which relies on an incremental approach that assumes an elastic behavior of the bare

structure during the design phase, and validates the damper design using a fully inelastic model at the end of the design process. In order to extend this method to include inelastic behavior during the design phase, or to compute fragility curves for the risk analysis, several inelastic analyses are required for the design and/or validation process. One option is to use Pushover analysis, but results are strongly dependent on the lateral load pattern and it is not straightforward to correctly include the effect of higher modes and lateral-torsional coupling. Ideally, the result of inelastic analyses should be response histories [4]. However, there is a tradeoff between precision and efficiency, thus, compromising realistic outputs versus a practical implementation, especially when studying a large set of buildings. As a consequence, both approaches seems rather unpractical.

1.2 A proposed solution for this issue

A feasible solution for the described problem is to find a model with a reasonable balance between accuracy and computational time requirements. This implies to define a base-case model considered as the "exact" case, and then calibrate a simpler model. This article is the first part of a bigger research that aims to use the results in a set of automated routines. Thus, to fully understand the associated problems, and for the sake of simplicity, let us consider first a simple structural configuration, i.e., plane and regular reinforced concrete moment resisting frames. In order to analyze realistic buildings, the structures will be designed according to the American ACI318-14 [5] and Chilean NCh433 codes [6,7,8]. Also, OpenSees [9] will run all the simulations and MATLAB [10] will be used to handle the data, since both are well-known computational frameworks with validated models, algorithms, integrators, and data analysis tools. Having this in mind, a research question arises: would it be possible to estimate the inelastic dynamic response of plane and regular R/C moment resisting frames in a significantly more efficient way relative to the base case, but without compromising accuracy of the outputs too much?. In response to this question, the hypotheses are that: (1) it is possible to calibrate a simplified MDOF nonlinear model, so that it is efficient —with a difference of at least one order of magnitude in the computation time— and accurate —capable of estimating the response-history of a set of interest variables (e.g., story displacements and base shear) with acceptable errors in the peak response (ideally 30% or smaller); and (2) the calibration can be performed with a set of simple analyses of the original case model. To accomplish the proposed solution, it is assumed that a force-based fiber model represents well the inelastic behavior of the selected structural configuration. The selected simplified model corresponds to the Modified Fishbone Model [11, 12], described in the next section. A procedure for calibrating the simplified model based on an optimization scheme will also be presented. Otherwise, the methodology is not practical.

2. Detailed and simplified models

2.1 Force-based fiber model for reinforced concrete elements

Usually, an inelastic dynamic analysis considers obtaining an equation of motion and integrating it numerically through a quadrature technique. This implies evaluating the constitutive relationships in different points along the elements and summing the results with adequate weights. Specifically, a Gauss-Lobato quadrature scheme will be used herein because it considers points located on the edges of the element, where the most significant nonlinearities are expected to occur. As a consequence, a reinforced concrete member has to be discretized in several cross-sections —selected to be consistent with the number and locations of the Gauss-Lobato quadrature points— and then each cross-section must be discretized in sufficiently small elements, the so-called fibers, to integrate the equations numerically. Each fiber has a uniaxial inelastic stress-strain constitutive relationship, which allows to consider different materials (like concrete and steel) in the same section, and a natural interaction between axial force and moment, because fibers work in the axial direction. Each section also considers an inelastic model for shear and an elastic model for torsion, which are aggregated to the axial/flexural section as explained elsewhere [13]. In summary, the element is based on a flexibility formulation —which means that a distribution is assumed for the moment diagram instead of a curvature diagram— allowing to use one element per structural member with good accuracy. An iterative scheme presented elsewhere [13, 14] is needed for the state-determination stage, since the global model is displacement-based and the element model is force-based.

Most fibers in a section will correspond to concrete, either core (confined) or cover (unconfined). To represent the behavior of this material, the Kent-Park model [15] will be used, modified to neglect tension and in-cycle degradation [13]. The mechanical properties of the material are determined based on the level of confinement, according to the expressions presented by Mander [16], which modify the strength, stiffness, and deformation capacity of concrete. For the implementation in OpenSees [9], the *Concrete01* uniaxial material was used, although it was slightly modified to make it consistent with the expressions given by Mander. The modification implies that the Young modulus is an input parameter instead of being computed from the stress and strain associated with the peak capacity. Also, the residual stress was set as $f_r = 0.2f_c^{'}$ for confined concrete and as $f_r = 0$ for cover concrete to consider spalling. For this model, an important parameter is the compressive fracture energy, because it is used in the energy-based regularization process of the fibers. For unconfined concrete, the value was obtained as presented elsewhere [13]; while for confined concrete, the energy was computed from numerical experiments. When it comes to steel, the model considers a piece-wise backbone curve with elastic behavior, a yield plateau, a hardening branch, and a softening branch, as well as a Menegotto-Pinto hysteresis rule. The model is capable of reproducing the Bauschinger effect, buckling and bar fracture, but not fatigue [13]. The buckling length is computed for each reinforcement bar considering the procedure of Dhakal and Maekawa [18].

2.2 The Modified Fishbone Model

This simplified model was proposed by Nakashima [11] to represent the behavior of plane and regular steel Moment Resisting Frames (MRF). As shown in Fig. 1, it replaces all the columns of a story with one equivalent macro-column and all beams of a story with a pair of equivalent macro-beams. Both macro-elements are elastic members with plastic end hinges that consider a trilinear force/deformation constitutive relationship. The model was later modified by Khaloo [12], who changed some assumptions and added a pair of elastic vertical trusses per story aimed to capture the effect of the external columns reaction that provide the overturning moment. This addition allows the model to represent the flexural drift of the MRF due to axial deformation of the columns.

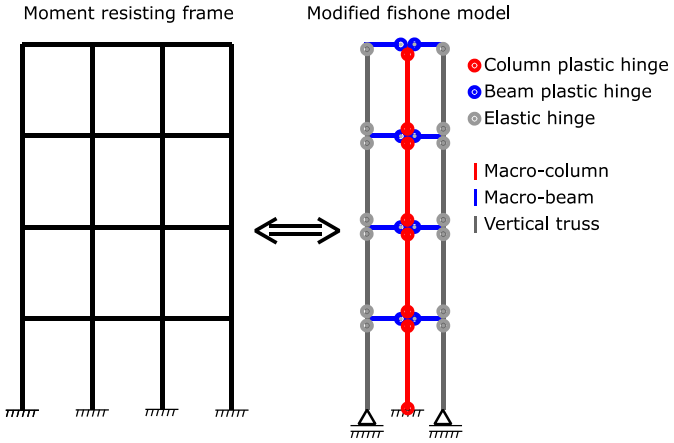

Figure 1: Moment resisting frame and Modified fishbone model

To build this model, it is necessary to compute the stiffness of the elastic elements —macro-beams, macro-columns and trusses— and the capacity of the inelastic rotational springs located at the ends of the macro-elements. The stiffness of the inelastic springs can be computed directly from the properties of the elastic macro-elements. To compute the required parameters, some assumptions on the MRF are required: (1) all the masses are lumped at the story level; (2) for columns, the rotation of all joints of a certain floor are the same; (3) for beams, the rotation of all interior joints are the same, while the rotations of exterior joints are slightly greater; and (4) only the exterior columns sustain the overturning moment, while the effect is neglected for the interior ones. With the second assumption, the kinematic constraint on the joint rotation of columns, it is possible to condense the columns of the MRF into the equivalent macro-columns of the MFB. In a similar way, it is possible to condense all the beams of the model into a pair of equivalent macro-beams [12]. Finally,

the axial stiffness of the equivalent trusses is computed so that the flexural interstory drifts of MRF and MFB are the same, as presented elsewhere [12]. The properties of the macro-elements are given by:

$$\boldsymbol{M_{cy}^{MFB} = \sum_{i=1}^{N_c} M_{cy,i}^{MRF}} \quad ; \quad \boldsymbol{EI_c^{MFB} = \sum_{i=1}^{N_c} EI_{c,i}^{MRF}} \tag{1}$$

$$\boldsymbol{M_{by}^{MFB} = \sum_{i=1}^{N_b} M_{by,i}^{MRF}} \quad ; \quad \boldsymbol{EI_b^{MFB} = \left[N_b - \frac{(N_b-1)(\alpha-1)}{N_b+1+2(\alpha-1)}\right] EI_b^{MRF}} \tag{2}$$

$$\boldsymbol{EA_i^{MFB} = \beta^2 EA_i^{MRF}} \tag{3}$$

where, for a given a story, M_{cy}^{MFB} and $M_{cy,i}^{MRF}$ are the capacities of the macro-column of the MFB and of the i-th column of the MRF, respectively; M_{by}^{MFB} and $M_{by,i}^{MRF}$ are the capacities of each of the two macro-beams of the MFB and of the i-th beam of the MRF; EI_c^{MFB} and $EI_{c,i}^{MRF}$ are the flexural stiffnesses of the macro-column of the MFB and of the i-th column of the MRF; EI_b^{MFB} and EI_b^{MRF} are the flexural stiffness of the macro-beams and of the beams of the MRF; N_c and N_b are the number of columns and beams, respectively; α is the ratio of external to internal joint rotation; β is the ratio between the distance of external columns in the MRF and the distance of vertical trusses in the MFB; and EA_i^{MFB} and EA_i^{MRF} are the axial stiffnesses of the vertical trusses and of the external columns.

3. Proposed changes to the Modified Fishbone Model

As it was explained in the previous section, the MFB was proposed for steel moment resisting frames. However, it is desirable to exploit its capabilities to efficiently analyze reinforced concrete frames as well, and thus, some modifications are needed. The hypothesis is that, since the inelastic behavior of the MFB is located at the rotational springs, by changing their constitutive relationship it is possible to adapt the model for another material. For example, the piecewise linear constitutive relationship must be replaced with a smooth hysteretic model, because the moment-rotation ($M-\theta$) curves of the fiber model show a transition between elastic and plastic ranges. Also, since the role of pinching can be important in reinforced concrete members, it is necessary to include this effect on the hysteretic model. Finally, the model must consider evolving properties, which means that a set of strength and stiffness degradation rules have to be defined, because both concrete and steel will suffer damage over time. To ease the understanding of the proposed model, it will be explained in terms of the quantities used in the implementation with the MFB, moment M and rotation θ, instead of in terms of stress and strain.

In order to include the previously mentioned effects, the proposed $M-\theta$ constitutive relationship of the rotational springs is modeled with a hysteretic spring —with zero stiffness in the plastic range— in parallel with an elastic spring to model hardening. The hysteretic spring includes degradation of both stiffness and strength, implemented as modification factors that will multiply and reduce the initial values. These factors use the maximum deformations and the dissipated energy to measure damage. Hence, the state vector of the model are given by $y = [\theta, M_{hys}, \theta_{max}^{+}, \theta_{max}^{-}, H]$, where θ is the rotation; M_{hys} is the hysteretic moment; θ_{max}^{+} and θ_{max}^{-} are the maximum and minimum rotations in the history of the element, respectively; and H is the dissipated energy. The proposed model was programmed in C++ and implement in OpenSees as a new uniaxial material in a DLL extension. The internal state-determination of the material is carried out using the classic RK4 integrator to obtain an initial guess, followed by a Newton-Raphson correction scheme until the error in the hysteretic moment is negligible.

3.1 Smooth hysteretic model

Instead of a piecewise linear backbone curve, the inelastic rotational springs of the MFB are assumed to follow a smooth hysteretic model. This model is based on the general expression of the Bouc-Wen model, as presented by Sivaselvan and Reinhorn [19], but with some minor modifications. The equation that governs the relationship between the rotation θ and the hysteretic moment M_{hys} is given by:

$$\frac{dM_{hys}}{d\theta} = \left[A_0 - \left|\frac{M_{hys}}{M_{hys_y}}\right|^N \left(\beta - sgn\left(M_{hys}\Delta\theta\right) + \gamma\right)\right] h\left(M_{hys}, \theta\right) K_{hys} \tag{4}$$

where M_{hys_y} is the capacity; N is a parameter that controls the sharpness of the transition between elastic and plastic ranges; A_0, β and γ are parameters that control the shape of the hysteresis; $h(M_{hys}, \theta)$ is the pinching function; and K_{hys} is the elastic stiffness. Both the capacity and stiffness are defined to consider degradation, $M_{hys_y} = R_m M_{hys_{y0}}$ and $K_{hys} = R_k K_{hys_0}$, where $M_{hys_{y0}}$ is the initial capacity; R_m is the strength degradation factor; K_{hys_0} is the initial elastic stiffness; and R_k is the stiffness modification factor to account for degradation. Both the stiffness and strength modification factors depend on the maximum deformations in the past and on the dissipated energy.

3.2 Pinching rules

When analyzing the behavior of reinforced concrete elements with the force-based fiber model, it was noted that the pinching effect was particularly strong. It was observed that the tangent stiffness is smoothly lost in the unloading branches, while in the reloading ones it is suddenly regained only near $\theta \approx 0$, even when unloading from very large deformations. It was not possible to reproduce this effect with existing pinching functions, because these models regain stiffness very smoothly, and because this transition may occur for very large values of rotation. Thus, it became necessary to propose a new pinching function capable of reproducing the observed effects, as explained elsewhere [20].

3.3 Strength and stiffness degradation rules

After analyzing the outputs of a series of pushover analyses of the fiber model, it was concluded that for the studied cases the stiffness degradation is mostly related to ductility, while the effect of dissipated energy can be neglected. Hence, the stiffness modification factor, R_k, is defined as a function of the maximum rotation in the past, θ_{max}. To improve the fitting and to ease the identification process, this function is assumed to be a tetralinear curve. It was observed that the initial branch is particularly important, because it captures the sudden loss of stiffness due to the initial cracking of concrete. If this effect is ignored, or incorrectly captured, the MFB does not behave properly for low demands. In order to consider cracking in both directions, the R_k factor is computed independently, for both, positive and negative deformations. Once again, ignoring this effect introduces error for low demands and for the initial cycles of the response-history analyses. By studying the same set of pushover analyses as before, it was observed that strength degradation depends on both the maximum rotation in the past, θ_{max}, and dissipated energy, H. Hence, a modification factor R_m is defined as a function of the Park and Ang damage index [21] to combine both effects. Like in the previous case, the degradation function that defines the R_m modification factor is computed for the positive and negative capacities and is assumed to follow a tetralinear curve.

4. Calibration of the simplified model

In order to select the optimal parameters of the simplified model, relative to the fiber model, a set of pushover analyses was carried out. The expressions proposed in the previous chapter were fit to this data by means of an optimization approach. Since a considerable number of parameters must be calibrated, the method follows a cascading algorithm. A combination of the Particle Swarm Optimization and Nelder-Mead algorithms are considered for this purpose, aggregating the contributions of different authors, as well as some new suggestions. In summary, these algorithms were selected to obtain a good balance between exploitation and exploration capabilities, to avoid getting trapped in local optima, and to get a good rate of convergence with a reasonable computational demand.

4.1 Particle Swarm Optimization / Nelder-Mead algorithm

The Particle Swarm Optimization (PSO) method was proposed by Kennedy and Eberhart [22] and was inspired by the social behavior of a school of fish (or a flock of birds). As many metaheuristics, PSO works with a set of candidate solutions, called particles, to enhance the exploration capabilities of the method and make it a derivative-free one. Essentially, it emulates how the members of a swarm benefit from both their own knowledge and that of the group, because a common effort is beneficial for the group. The same idea is generalized in an abstract way and then applied to optimize a nonlinear problem. For example, suppose you

want to identify the parameters of a smooth hysteretic model so that its response fits some experimental data. The fitness function to be minimized may be the cumulative square error between the target hysteresis and the one obtained with the proposed smooth hysteretic model. In the same way, each candidate solution —or particle— will be a vector $\boldsymbol{x}$ containing the parameters of the simplified model —stiffness, strength, shape and degradation parameters, among others. The algorithm tests the particles and updates them at each iteration, attempting to improve them.

The Nelder-Mead (NM) algorithm was proposed in 1965 [23] and many variations have been proposed since then. It is a comparative optimization algorithm that works with a simplex of candidate solutions, which is a polyhedron of $(n + 1)$ points if the problem is n-dimensional. It is a derivative-free method that updates the simplex of candidate solutions at each step as an attempt to replace the worst point with a new and better one. This is performed by using four basic actions —reflection, expansion, contraction and shrink— until convergence is achieved, as presented elsewhere [24].

In this research, both PSO and NM algorithms were combined and implemented in MATLAB to conduct the optimization. The NM method is introduced inside the PSO algorithm and after it has converged, giving the procedure more exploitation capabilities. This allows to work with higher velocities in PSO, covering all the search domain efficiently, but with a good rate of convergence. In essence, just before updating the velocity of the particles, the Nelder-Mead algorithm is called. It takes the best particle of the swarm and builds a simplex with it and N_d random perturbations of it, where N_d is the dimension of the particle. After building the simplex, the Nelder-Mead algorithm is applied. Once the process has finished, the best particle of the swarm is replaced with the best particle of the simplex.

4.2 Parameter identification of the Modified Fishbone Model

The parameters of the simplified model are identified from the results of a set of pushover analyses of the structure. There are several ways of doing so, and after testing different approaches, the one that proved to work best is based on the work of Wang et al [25]. First, the plastic hinge length of each element is computed, based on the procedure presented by Dides [26]. Then, a cascading algorithm identifies one set of parameters at a time. The identification itself is carried out by expressing the problem in an optimization format and using the PSO-NM algorithm, as has been done before by others [27]. In all cases, the fitness function is computed as the sum of the square error between the data points from the pushovers and those of the candidate solution. The cascading nature of the process ensures that the complete set of parameters is identified quickly, because the optimization problems are low-dimensional in nature.

5. Validation

5.1 Benchmark structures

In order to validate the proposed simplified model, a set of moment resisting frames with 1, 5, 10, 15 or 20 stories, and with 3, 6 or 9 bays was used. The buildings are designed according to the American ACI318-14 [5] and Chilean NCh433 [6,7,8] codes. All the elements, beams or columns, of a certain group of consecutive stories share the same cross-section geometry, reinforcement, and concrete type. Each frame was subject to a set of response-history analysis considering a consistent set of ground motions. The peak responses were stored for the story displacements and base shear, for both the MRF and the MFB models. This data was used to compute the average and standard deviation of the responses of both models, as well as the relative error with respect to the fiber model. Also, to measure the performance of the MFB, the computation time required to run all the simulations was stored for both the original and the simplified structural models.

5.2 Selection of a consistent set of seismic records

The structural response for a given level of spectral acceleration at a period of interest T^* can be predicted using dynamic analysis, which requires ground motions as inputs. The selection of these ground motions usually consists in matching a target response spectrum, and hence, requires computing the value of spectral accelerations at periods other than T^*. The Conditional Mean Spectrum (CMS), which represents the expected

spectrum conditioned on the occurrence of a given spectral acceleration at the period of interest, $S_a(T^*)$, is an appropriate target spectrum since it is probabilistically consistent with the seismic hazard of a site [28]. Constructing a CMS requires computing the conditional mean of the logarithm of a spectral acceleration at other periods T. Spectral accelerations at periods other than T^* also present variability, which can be represented by the conditional standard deviation. The CMS is the exponential of the conditional mean, and represents the median value of $S_a(T)$ given a value of $S_a(T^*)$. If a spectrum also considers the conditional standard deviation, it is termed Conditional Spectrum (CS), and together with the conditional mean defines a lognormal distribution for spectral accelerations at any period [29].

For this research, candidate ground motions for selection were obtained from a recently compiled database of Chilean strong motion records, SIBER-RISK [30], and were first scaled to match the target spectral acceleration at the conditioning period. The ground motions were selected for a site in the city of Santiago, Chile, with an average shear wave velocity in the top 30 m of soil (V_{s30}) of 425 m/s. A conditioning period of 1 s was used since it is approximately the average fundamental period of the structures considered in the analysis. An exact implementation of the Conditional Spectrum was computed for 10 levels of spectral accelerations at the conditioning period linearly spaced between 0.1 g to 1.0 g, which correspond to return periods ranging from 41 to 3400 years. At each intensity level, 50 ground motions were selected to match the mean and variance of the CS over a period range between 0 and 4 s using the algorithm proposed by Jayaram et al. [31]. The PSHA at the site was performed using the seismic source model proposed by Poulos et al. [32] for Chilean subduction earthquakes and the GMPE proposed by Abrahamson et al. [33]. The correlations between spectral accelerations at different periods were computed using the model proposed by Baker and Jayaram [34]. The method that was used herein to compute CS was the aggregation approach to the "exact" method proposed by Lin et al. [29], which combines the contribution of all possible earthquakes considered during a Probabilistic Seismic Hazard Analysis (PSHA), and hence does not rely on deaggregation.

5.3 Results

For each building, the comparison of the MRF and MFB models is performed on a story-by-story basis. For space considerations, this section only presents results for roof displacement and base shear, and for structures with 3 bays, but similar results are obtained for other stories and for different number of bays [20]. The peak roof displacements are compared in Figure 2, while the peak base shear are compared in Figure 3. In both cases, subfigures are used to display the results for structures with 1, 5, 10, 15 and 20 stories. In general, in the first half of the subfigures the mean responses are shown in a solid line, while a band of one standard deviation is represented in discontinuous lines. The results are shown in blue lines for the MRF and in orange lines for the MFB. In the second half of the subfigures, the relative error in mean responses is displayed.

From the results of Figure 2 it is apparent that the error in the mean responses of roof displacements is small, especially for intensities bigger than 0.3g. It is usually smaller than 20% and oscillates around zero. The figure also shows that the standard deviation of peak roof displacement is estimated quite accurately. The errors tend to be smaller than 40%, except for the 20-story MRF, where the dispersion is much bigger for small intensities, since more members remain elastic. When it comes to base shear, the results are less accurate, but are still acceptable, as shown in Figure 3. The mean peak values are estimated with reasonable accuracy for intensities greater than 0.3g. For these cases, the relative error is smaller than 20%, converges to zero and tends to overestimate the response. With respect to the standard deviation, larger errors are observed. The results obtained in other stories and number of bays show that, in general, larger errors are obtained for low intensity demands. Some analyses show that the errors are due to an inadequate correction of the stiffness of the elastic macro-elements. Hence, in order to improve the results, a more robust approach —like the one presented by Dides [27]— is required. In any case, it should be noticed that the model presents the biggest errors in the cases that have the least significance. When the structure undergoes strong inelastic behaviour, the model is more accurate; it is for these cases that the MFB is really useful and will be used to evaluate the building behaviour.

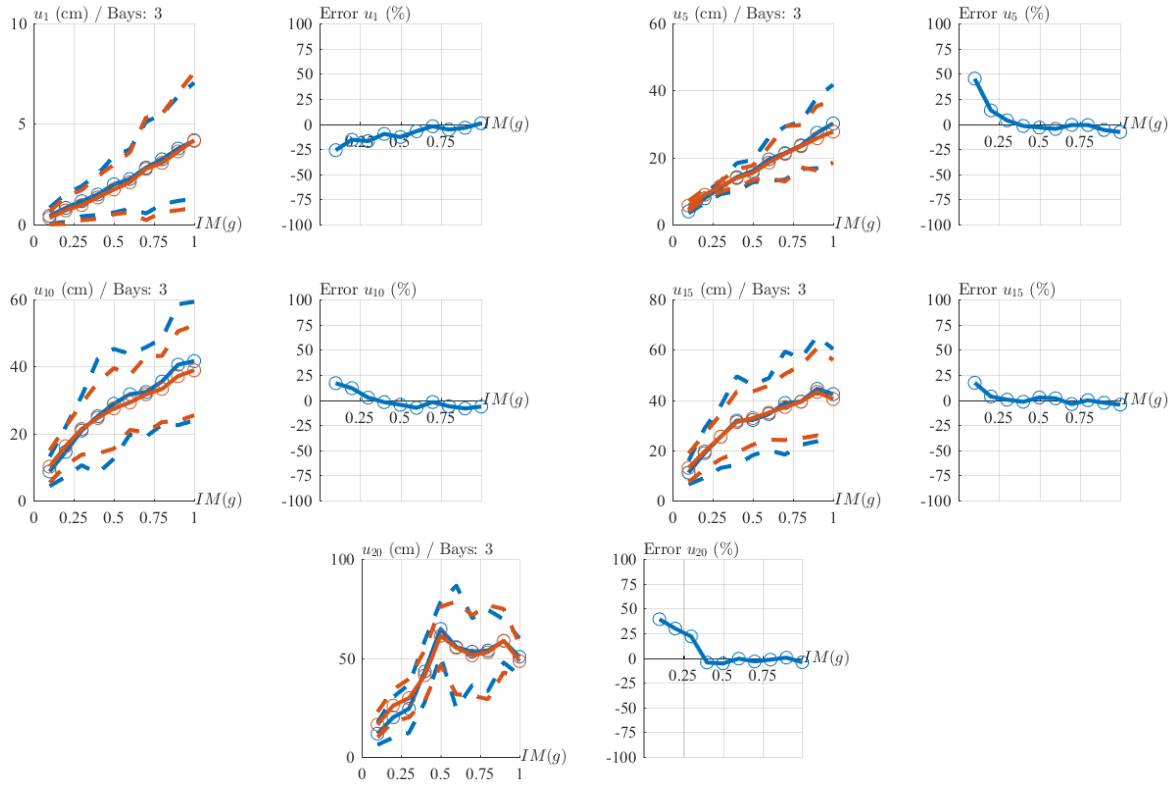

Figure 2: MRF (blue) and MFB (orange) comparison of roof displacement, for 1, 5, 10, 15 and 20 stories, and 3 bays

It was noted that the simplified model requires approximately 10 times less computation time than the MRF for the structures with 3 bays —except for the single-story case, were the ratio is 5. Moreover, when adding bays, the number of inelastic elements increases in the MRF, and so it does the required computational time. However, the MFB always have the same number of inelastic elements, no matter the number of bays. As a consequence, the model becomes even more efficient relative to the MRF for structures that grow in number of bays, requiring approximately 20 and 30 times less computation time than the MRF for the structures with 6 and 9 bays, respectively. Naturally, the MRF can be forced to be more efficient if a coarser discretization is used, but it was observed that it tends to cause problems in convergence, and the efficiency gain was not that important. For example, the MFB was 8 times faster, instead of 10, when a constant discretization of forty layers was used for all the elements.

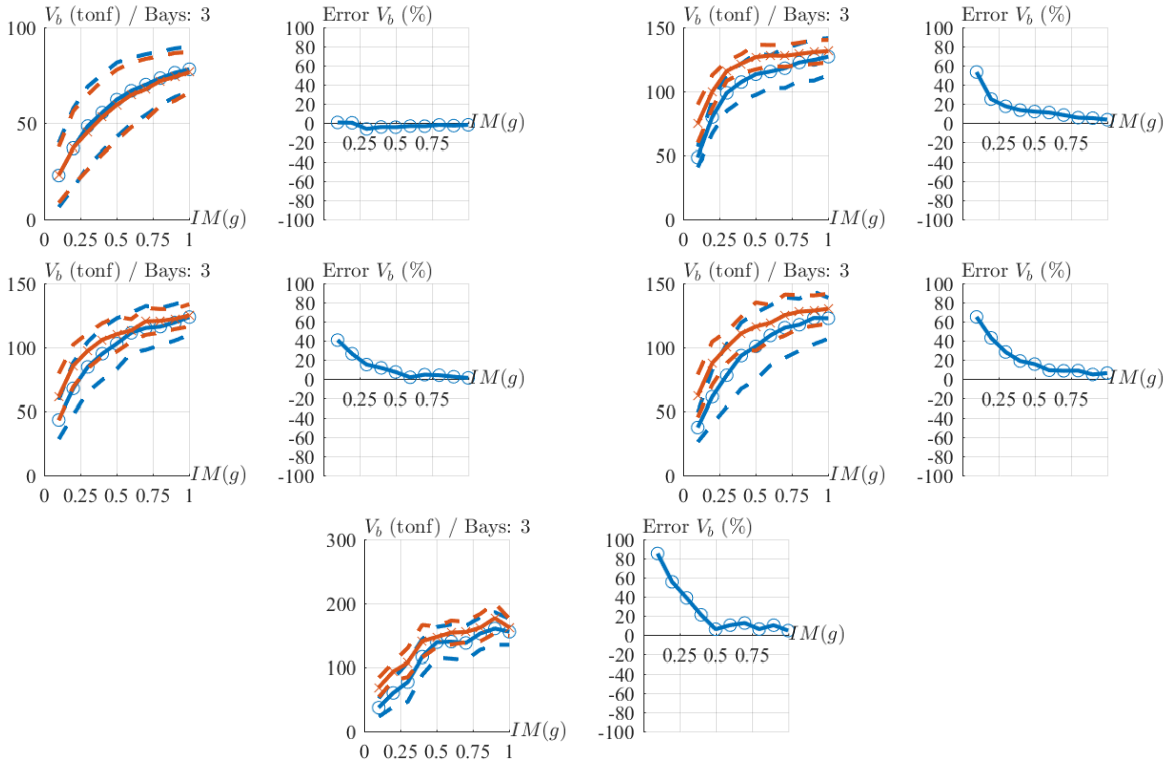

Figure 3: MRF (blue) and MFB (orange) comparison of base shear for 1, 5, 10, 15 and 20 stories, and 3 bays

6. Conclusions

A cascading methodology for calibrating the parameters of the simplified MFB model was presented based on an optimization scheme. The simplified model can predict the peak responses of story displacement and base shear of the original structural model with good accuracy, while requiring between 5 and 30 times less computational time. In most cases, the errors in the predictions are below 20% and 40% for the mean response and its standard deviation, respectively. Only for very low intensities, the proposed model tends to overestimate the inelastic response by larger factors, sometimes with errors between 60% and 100%. It was observed that this issue can be corrected easily and is not important for the cases where the simplified model will be used, which is for strong ground motions. Also, since the displacements are correctly estimated in all the stories, the MFB can be used to effectively predict the distribution of damage in height, for instance to design Energy Dissipation Devices, or to evaluate the performance of the building and its non-structural components, both, for new and existing structures.

7. Acknowledgments

This research has been sponsored by different research grants, Fondecyt grant 1170836 and Fondap grant 15110017. The authors are thankful for this support. Also, the authors would like to thank Dr. Marco Baiguera of UCL for his useful comments, and CONICYT for funding the MSc studies of the principal author (CONICYT-PFCHA/Magíster Nacional/2018-22180377).

8. Copyrights

9. References

1. Vásquez A., Rivera F., de la Llera J. C., Mitrani-Reiser J. Healthcare network's response and resilience in Iquique after the 2014, Pisagua earthquake; 2017.
2. Cimellaro G. P., Reinhorn A. M., Bruneau M. Seismic resilience of a hospital system. Structure and Infrastructure Engineering, 2010; 6(1-2): 127–144. doi: 10.1080/15732470802663847
3. de la Llera J. C., Muñoz J.P., Besa J. J. A design procedure for buildings equipped with energy dissipation devices using nonclassical damping and iso-performance curves. Earthquake Engineering and Structural Dynamics 2019; 45: 210–231.
4. Maniatakis C., Psycharis I., Spyrakos C. Effect of higher modes on the seismic response and design of moment-resisting RC frame structures. Engineering Structures 2013; 56: 417–430.
5. American Concrete Institute. Requisitos de reglamento para concreto estructural (ACI 318S-14) y comentario. 2014.
6. Instituto Nacional de Normalización. Diseño sísmico de edificios, NCh433.Of1996, Instituto Nacional de Normalización; Santiago. 2009.
7. Instituto Nacional de Normalización. Decreto Supremo 61, Instituto Nacional de Normalización; Santiago. 2011.
8. Instituto Nacional de Normalización. Decreto Supremo 60, Instituto Nacional de Normalización; Santiago. 2011.
9. Mazzoni S., McKenna F., Scott M. H., Fenves G.L. OpenSees [Computer Software]: The Open System for Earthquake Engineering Simulation. 2013.
10. The Math Works Inc . Matlab 2017b. 2007.
11. Nakashima M., Ogawa K., Inoue K. Generic frame model for simulation of earthquake responses of steel moment frames. Earthquake Engineering and Structural Dynamics 2002; 31(3): 671–692. doi: 10.1002/eqe.148
12. Khaloo A., Khosravi H. Modified fish-bone model: A simplified MDOF model for simulation of seismic responses of moment resisting frames. Soil Dynamics and Earthquake Engineering 2013; 55: 195–210.
13. Vásquez J., de la Llera J. C., Hube M. A regularized fiber element model for reinforced concrete shear walls. Earthquake Engineering and Structural Dynamics 2016; 45(13): 2063–2083. doi: 10.1002/eqe.2731
14. Spacone E., Fiippou F., Taucer F. Fibre beam-column model for non-linear analysis of R/C frames: Part I. Formulation. Earthquake Engineering and Structural Dynamics 1996; 25: 711–725.
15. Scott B., Park R., Priestley M. Stress-Strain Behavior of Concrete Confined By Overlapping Hoops At Low and High Strain Rates. Journal of the American Concrete Institute 1982; 79(1): 13–27.
16. Mander J., Priestley M., Park R. Theoretical stress-strain model for confined concrete. Journal of Structural Engineering (United States) 1988; 114(8): 1804–1826. doi: 10.1061/(ASCE)0733-9445(1988)114:8(1804)
17. Mazzoni S., McKenna F., Scott M., Fenves G., Others. OpenSees command language manual. Version 2.5.0. tech. rep., 2005.
18. Dhakal R., Maekawa K. Reinforcement stability and fracture of cover concrete in reinforced concrete members. Journal of Structural Engineering 2002; 128(10): 1253–1262. doi: 10.1061/(ASCE)0733-9445(2002)128:9(1186)
19. Sivaselvan M., Reinhorn A. Hysteretic models for deteriorating inelastic structures. Journal of Engineering Mechanics 2000; 126(6): 633–640.
20. Muñoz, J.P. An automatically calibrated simplified model for efficient inelastic dynamic analysis of plane and regular reinforced concrete moment resisting frame. MSc Thesis. 2019; Pontificia Universidad Católica de Chile
21.Park Y., Ang A. Mechanistic seismic damage model for reinforced concrete. Journal of Structural Engineering 1985; 111(4): 722–739.
22. Kennedy J., Eberhart R. Particle Swarm Optimization. 1995: 1942–1948.
23. Nelder J., Mead R. A Simplex Method for Function Minimization. The Computer Journal 1965; 7(4): 308–313. doi: 10.1093/comjnl/7.4.308
24. Lagarias J., Poonen B., Wright M. Convergence of the restricted Nelder-Mead algorithm in two dimensions. SIAM Journal on Optimization 2012; 22: 501–532.

25. Wang P., Ou Y., Chang K. A new smooth hysteretic model for ductile flexural-dominated reinforced concrete bridge columns. Earthquake Engineering and Structural Dynamics 2017; 46: 2237–2259.
26. Dides M., de la Llera J. C. A comparative study of concentrated plasticity models in dynamic analysis of building structures. Earthquake Engineering and Structural Dynamics 2005; 34: 1005–1026.
27. Moravec P., Rudolf P. Combination of a Particle Swarm Optimization and Nelder-Mead Algorithm in a Diffuser Shape Optimization. Advances in Hydroinformatics 2018: 997–1012.
28. Baker J. Conditional mean spectrum: Tool for ground-motion selection. Journal of Structural Engineering 2011; 137(3): 322–331. doi: 10.1061/(ASCE)ST.1943-541X.0000215
29. Lin T., Harmsen S., Baker J., Luco N. Conditional spectrum computation incorporating multiple causal earthquakes and ground-motion prediction models. Bulletin of Seismological Society of America 2013; 103(2A): 1103–1116.
30. CIGIDEN. SIBER-RISK: Strong motion database. 2019.
31. Jayaram N., Lin T., Baker J. A Computationally efficient ground-motion selection algorithm for matching a target response spectrum mean and variance. Earthquake Spectra 2011; 27(3): 797–815. doi: 10.1193/1.3608002
32. Poulos A., Monsalve M., Zamora N., de la Llera J. C. An Updated Recurrence Model for Chilean Subduction Seismicity and Statistical Validation of Its Poisson Nature. Bulletin of Seismological Society of America 2019; 109(1): 66–74.
33. Abrahamson N., Gregor N., Addo K. BC Hydro ground motion prediction equations for subduction earthquakes. Earthquake Spectra 2016; 31(1): 23–44.
34. Baker J., Jayaram N. Correlation of spectral acceleration values from NGA ground motion models. Earthquake Spectra 2008; 24(1): 299–317. doi: 10.1193/1.2857544

